



Prediction of knot size in uneven-sized Norway spruce stands in Sweden

N. Fagerberg^{a,*}, S. Seifert^b, T. Seifert^{c,g}, P. Lohmander^a, A. Alissandrakis^d, B. Magnusson^e, J. Bergh^a, S. Adamopoulos^f, M.K.-F. Bader^a

^a Department of Forestry and Wood Technology, Linnaeus University, 351 95 Växjö, Sweden

^b SCIMOND Scientific Services, Ruppertskirchen 5, 85250 Altomünster, Germany

^c Chair of Forest Growth and Dendroecology, Albert-Ludwigs-University Freiburg, Tennenbacher Str. 4, 79106 Freiburg, Germany

^d Department of Computer Science and Media Technology, Linnaeus University, 351 95 Växjö, Sweden

^e Department of Building Technology, Linnaeus University, 351 95 Växjö, Sweden

^f Department of Forest Biomaterials and Technology, Swedish University of Agricultural Sciences, Box 7070 750 07, Uppsala, Sweden

^g Department of Forest and Wood Science, Stellenbosch University, 7602 Matieland, South Africa

ARTICLE INFO

Keywords:

Branch model
Stem quality
Uneven-aged
Picea abies
Continuous cover forestry
Crown shape

ABSTRACT

The size of knots is negatively correlated with bending strength in sawn timber and it is therefore used as a quality grading criterion in national roundwood grading standards. Some standards even use the size of the largest knot as the sole estimate for individual log knottiness. The size of knots is determined by crown horizontal extension, which in turn is dependent on the impact of competing trees. Thus, with knot size models that are competition-dependent, roundwood quality due to knottiness can be simulated for different management alternatives. However, these types of models, calibrated on uneven-sized Norway spruce in Fennoscandia, are currently not available. Therefore, the objective of this study is to develop a competition-dependent model framework for prediction of the largest knot size per stem height section, for application within uneven-sized Norway spruce stands. Data from terrestrial laser scanning of an uneven-sized stand in southern Sweden are used to calibrate a modular prediction framework, consisting of interlinked allometric statistical models. Alternative framework sub-models are presented and the preferred model combination can be selected according to context and available input data. The flexible modular format enables further development of separate sub-components for adaptation to growing conditions not covered by the current calibration range.

1. Introduction

The size of knots is decisive for strength of structural timber. In fact, the cross-sectional surface area of a knot can, in terms of material strength, be considered as a hole since it has no load-carrying capacity under tension (Mitsuhashi et al., 2008; Williams et al., 2000). In addition, grain directions in the clear wood surrounding the knots deviate from the stem axis direction, which further reduce the overall bending strength and affect stiffness (Johansson, 2003; Macdonald & Hubert, 2002; Oscarsson et al., 2012). The size of knots is therefore negatively correlated with bending strength in sawn timber (Baño et al., 2013; Johansson, 2003). Due to this, knot size has long been used for determining wood quality in roundwood grading (Colin & Houllier, 1991; Houllier et al., 1995; Moberg, 2006) and is therefore generally included

in national grading standards (e.g. Björklund, 2021). In Swedish standards for roundwood grading of softwood, the size of the largest knot is even used as the sole estimate of individual log knottiness (Anon, 2014).

In this study (and in the Swedish grading standards), knot size is defined as the branch diameter along the stem axis, at stem surface, excluding bark and collar. Branch diameter is correlated with crown horizontal projection (Deleuze et al., 1996; Seifert, 2003), which in turn is dependent on the impact of competing trees (Madgwick et al., 1986; Seifert, 1999) and the size of the tree itself (e.g. Johansson, 1992; Vestøl et al., 1999). The sizes of branches are further related to the distance from the top of the tree (Mäkinen et al., 2003), since older branches that have had more time to grow are located further down the canopy. At a certain distance from the top, estimated to approximately 5 m by Kantola and Mäkelä (2004), inter-tree competition starts to influence

* Corresponding author.

E-mail addresses: nils.fagerberg@lnu.se (N. Fagerberg), s.seifert@scimond.com (S. Seifert), thomas.seifert@wwd.uni-freiburg.de (T. Seifert), Peter@Lohmander.com (P. Lohmander), aris.alissandrakis@lnu.se (A. Alissandrakis), benganmagnusson@gmail.com (B. Magnusson), johan.bergh@lnu.se (J. Bergh), stergios.adamopoulos@slu.se (S. Adamopoulos), martin.bader@lnu.se (M.K.-F. Bader).

<https://doi.org/10.1016/j.foreco.2023.121206>

Received 22 February 2023; Received in revised form 9 June 2023; Accepted 11 June 2023

Available online 26 June 2023

0378-1127/© 2023 The Author(s). Published by Elsevier B.V. This is an open access article under the CC BY license (<http://creativecommons.org/licenses/by/4.0/>).

Table 1
Simontorp site description.

Latitude (°)	56°21
Altitude (m)	120
Site index (SI) ^a	G31
Number of stems (st ha ⁻¹)	612
Stand basal area (m ² /ha)	30
Mean tree diameter at breast height (mm)	221
Proportion of Norway Spruce	0.74
Self-thinning ratio ^b	0.05

^a SI = height at age 100, according to the Swedish system (Hägglund and Lundmark 1977).

^b Self-thinning ratio represents number of trees that have died within the last 10 years divided by number of living trees.

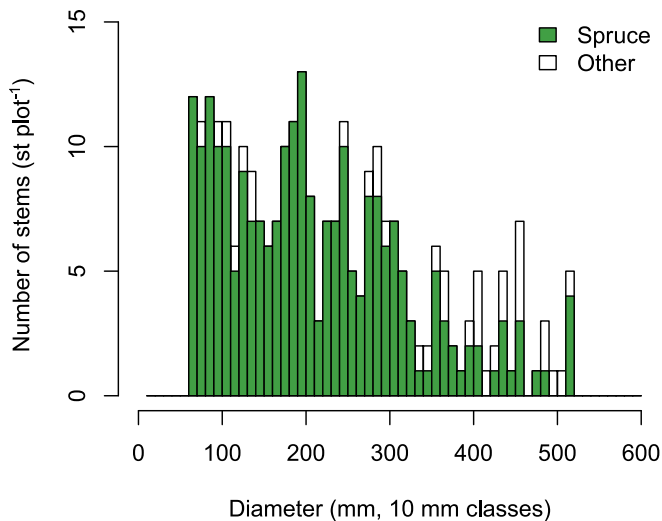


Fig. 1. Diameter distribution of the Simontorp stand (60 × 60 m). Only trees with diameter at breast height above 60 mm are included. Other tree species are mainly represented by Scots pine.

branch development with increasing effect until it finally causes branches to die (Colin & Houllier, 1991; Seifert, 2003). Even without inter-tree competition the growth of the lower branches is reduced (Colin & Houllier, 1991; Deleuze et al., 1996). Also the azimuthal orientation (Moberg, 2006; Rouvinen & Kuuluvainen, 1997; Skatter & Kucera, 1998) and inter-tree canopy contacts (Mitchell, 1975; Ottorini, 1991) impose physical restrictions on light availability, which affects crown extension. The resulting individual knot size is trigonometrically related to the branch angle, which in turn is related to branch age (Seifert, 2003).

Silvicultural methods and the resulting stand structure affect crown morphology (Colin & Houllier, 1992; Hasenauer & Monserud, 1996). Only limited research has been carried out on branch development of Norway spruce within stands with heterogeneous tree-diameter distributions (i.e. uneven-sized stands), but some general effects have been described for other conifer species. Macdonald et al. (2009) found, by using model simulations of Sitka spruce, that transformation to an uneven-aged structure resulted in a reduced knot area ratio. The shape of crowns in uneven-sized stands vary depending on social position (Pretzsch & Rais, 2016) where large trees have longer relative crowns compared to even-aged stands (Bianchi et al., 2020a; Hasenauer & Monserud, 1996; Kumpu et al., 2020). Crowns of suppressed conifers in selection forests are wider than trees of the same size in even-aged stands (Gilmore & Seymour, 1997; Kern, 1966; Pretzsch & Rais, 2016; Schütz, 1997) but their branches remain smaller in diameter (Man & Lieffers, 1999).

A useful strategy to model knot sizes is to estimate branch diameter

as a function of branch length, after first simulating the shape of the crown (Colin & Houllier, 1991; Deleuze et al., 1996; Seifert, 1999). Moberg (2001) suggested that the shape of the living part of the crown mainly depends on current growing conditions and only insignificantly on past growth development, supporting the idea that present competition estimates could be sufficient for prediction of the branch lengths. This assumption can be expected to be more correct the more time has passed since the last thinning event. Branch age is another useful predictor of branch length, because annual distal growth is a decreasing function of age (Deleuze et al., 1996; Tamm & Mao-Yi, 1987). Branch age can be estimated based on models for height growth as a function of time (Deleuze et al., 1996; Fagerberg, 2021). By combining these types of allometric statistical relationships, a flexible framework for knot size can be built.

Previous research indicates that the relationships between local competition and crown extension estimates are often weak (Vieilledent et al., 2010). Although individual tree canopies show considerable variation in plasticity, isolating competition variables to explain the variation has proved challenging. Competition indexes based on symmetric interaction (Weiner & Thomas, 1986) tend to be less successful (Deleuze et al., 1996; Geburek et al., 2008), compared to indexes that describe asymmetric competition (Purves et al., 2007; Vincent & Harja, 2008). Hasenauer and Monserud (1996) presented significant correlations with asymmetric local competition indexes i.e. basal area of larger trees and crown competition factor (Krajicek et al., 1961), for Norway spruce. Vieilledent et al. (2010) tested nine different competition indexes (symmetric and asymmetric) but could not show that crown height or crown radius of Norway spruce is associated with light or space availability. A contributing reason why it is difficult to isolate significant relationships for spruce is that shade-tolerant species show a weaker response to changed competitive conditions than shade-intolerant species (Grubb, 1998). An alternative to predict crown shape as a function of local competition is to directly use estimated crown length as a proxy for local competition impact (Colin & Houllier, 1991; Moberg, 2001) and based on that predict crown horizontal extension.

Knot size models for Norway spruce in Fennoscandia, which are adapted to uneven-sized structures, and additionally include impact from local competition, do not currently exist. Previous attempts to link local competition indicate that a stronger correlation can be achieved if the asymmetric relationships in the competition are included. The development of such a competition-dependent model for largest knot size would facilitate flexible simulations of silviculture impact on log grading quality.

The objective of this study is to develop a model framework for prediction of the largest knot size per stem height section depending on local competition, and for application within uneven-sized Norway spruce management.

2. Material and methods

2.1. Study site

Data were collected in an uneven-sized stand in southern Sweden, Simontorp, located in Östra Göinge (Table 1, Fig. 1). The stand consists almost exclusively of Norway spruce with Blueberry field vegetation type and Mesic soil moisture type (according to Swedish site index system, Hägglund & Lundmark, 1977). The site has never been clearcut and has a long history of multifunctional use where production of timber and firewood has been combined with grazing of livestock. Livestock grazing continued until the 1960s and active individual tree selective cuttings have been carried out since at least around 1950. Data were measured within a square plot of 60 × 60 m. The last selective thinning within the measured plot took place in 2005, and in 2007, when a few individual trees were windthrown. Three mature trees were harvested in 2014, close to the eastern border within the plot.

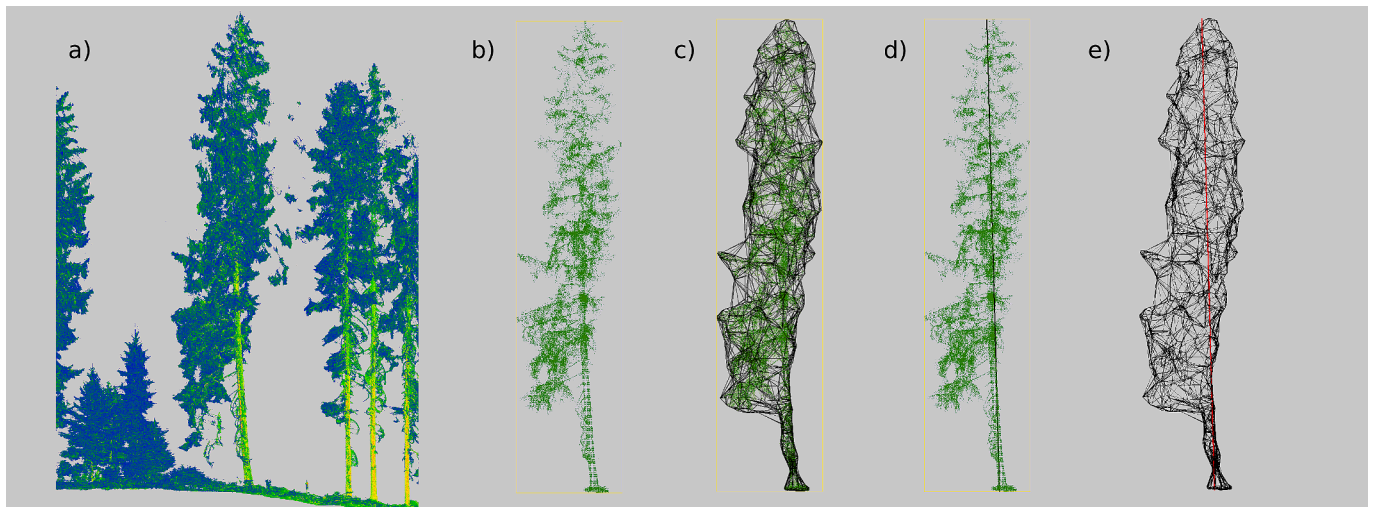


Fig. 2. Visual description of point-cloud data extraction of one example tree. a) original point shape (colours indicate the returned laser intensity.), b) manually extracted and simplified (filtered and voxelized) point shape, c) alpha shape on top of the simplified point shape, d) fitted stem axis on top of the simplified point shape, and e) fitted stem axis with alpha shape.

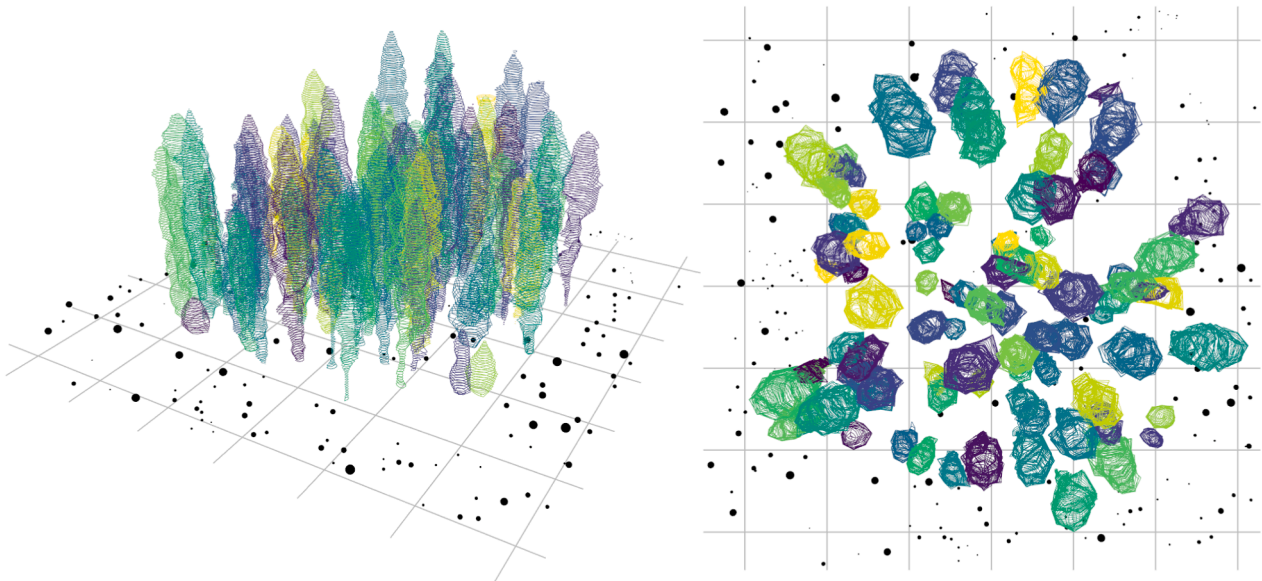


Fig. 3. Three-dimensional surface shapes of all the sample trees used in the combined data set. The shapes are described with octagons placed at 0.3 m height intervals. The colour palette is introduced to visually separate tree individuals. Black dots indicate size and positions of surrounding and mixed-up trees that did not qualify to be sample trees.

2.2. Data

Data collections were conducted during 2017 and 2018 and the final data set is a combination of two separate data sets, both with recorded tree positions but based on different measuring techniques, ultrasound and terrestrial laser. In the first data set (Postex data set), all trees above 60 mm diameter at breast height (D) were allocated spatial coordinates and cross-calipered with Postex ultra sonic equipment (Hagl f, Sweden). Coordinates were measured from nine circular sample plots evenly distributed in a grid. The nine sub-plots were inter-fitted into one global coordinate map by ordinary least square regression of double-measured coordinate reference points, defined by sticks placed along the sub-plot borders. Tree position measurement error was estimated to be 4 cm (one standard deviation). In a second round of the Postex data collection, additional data were collected from a sample of trees representative of

all diameter classes above 60 mm (see Fagerberg et al., 2022), with measurements including tree height (Th) and height to lowest living branch (Ch) (Vertex IV, Hagl f, Sweden). The same sample trees were also used for branch measurements, where all living branches that were possible to measure with a ladder from ground were included (approximately 5.5 m height). Horizontal branch diameter (d), branch insertion point height (h) and whorl ordinal number (W), were all recorded.

A separate branch data set (Reference tree data set) was also used to add information for estimating a function for branch diameter (d). These data were collected from four dominant trees with vital crowns that grew just outside the trial plot (see Fagerberg, 2021). These trees were felled, and two branches with opposite horizontal direction from the trunk were measured for each whorl where possible. Living branch data for branch insertion angle (α), branch insertion height (whorl heights) (h), branch age (A), horizontal branch diameter (d), and branch

Table 3
List of parameter designations and definitions.

Designation	Unit	Definition	Data	Framework function
α_h	(degree)	Angle between the horizontal plane and branch direction at insertion point (downward = positive)	Observation	Fagerberg (2021)
A_h	(years)	Branch age at height h	Prediction	$W_{Th} - W_h$
Bal_i	(m ²)	Sum of basal area of trees with larger Dbh than subject tree Dbh_i , within 8 m radius from tree i . Includes trees that have died within the last 10 years.	Observation	
Ch_i	(m)	Vertical distance between point of germination and branch insertion point of lowest living branch for tree i	Observation/ Prediction ^b	Fagerberg (2021)
CR_i		Crown ratio for tree i	Observation	$(Th_i - Ch_i)/Th_i$
D_{c_i}	(mm)	Diameter at breast height (1,3 m height) for competitor tree c_i in relation to subject tree i	Observation	
D_i	(mm)	Diameter at breast height (1,3 m height) for tree i	Observation	
d_h	(mm)	Horizontal branch insertion diameter at bark and at height h	Observation	see Results
L_h	(m)	Horizontal branch length from insertion to tip at height h	Observation ^c	see Results
HP_{ht}	(m)	Horizontal crown projection at height ht	Observation	
h	(m)	Vertical distance from ground to point of branch insertion	Observation ^a	
ht	(m)	Vertical distance from ground to point of branch tip	Observation	
Δh	(m)	Vertical distance from point of branch insertion to branch tip at height h	Prediction	Fagerberg (2021)
K_h	(mm)	Largest knot diameter at height h (excluding bark and collar, at insertion, parallel to stem axis)	Observation	see Equation (2)
R_{c_i}	(m)	Distance between subject tree i and competitor tree c_i	Observation	
r_h	(m)	Stem radius at height h , including bark thickness	Prediction	Edgren and Nylinder (1949)
rd_h		Relative vertical distance from	Observation	$(Th_i - h)/Th_i$

Table 3 (continued)

Designation	Unit	Definition	Data	Framework function
		treetop to branch insertion point at height h		
Th_i	(m)	Tree height for tree i	Observation	Fagerberg (2021)
W_h		Whorl ordinal number at height h	Prediction	Fagerberg (2021)
W_{Th}		Whorl ordinal number at tree height (tree age)	Prediction	Fagerberg (2021)

^a Observations calculated from ht plus predictions of Δh .

^b Observations from Postex sample trees (n = 62) and the remaining trees without observation data (n = 18) were predicted.

^c Observations calculated from HP_{ht} minus predictions of r_h .

Table 4

Statistics for horizontal branch length models a) Competition model ($L(Bal, .)$), b) Crown ratio model ($L(CR, .)$), and c) complex polynomial competition model ($pL(Bal, .)$). AIC = Akaike information criterion. $\alpha = 0.05$. fRMSE = root mean squared error of total sample fit, tRMSE = average of root mean squared error values from 10-fold cross-validation test samples. R^2_{adj} = adjusted R^2 .

	$L(Bal, .)$	$L(CR, .)$	$pL(Bal, .)$
Intercept	1.044	1.130	0.2911
Bal	-0.2216		-2.302
Bal^2			6.574
Bal^3			-4.705
$\ln(rd)$	0.8785	0.8249	
rd			10.19
rd^2			-18.04
rd^3			8.862
$\ln(A)$	0.1701		
h	0.1520	0.1442	-0.1773
h^2	-3.075e ⁻³	-3.723e ⁻³	1.020e ⁻²
h^3			-2.323e ⁻⁴
$D \times CR$		2.852e ⁻³	
D^2			5.792e ⁻⁵
D^3			-1.755e ⁻⁷
D^4			1.550e ⁻¹⁰
R^2_{adj}	0.604	0.657	0.732
fRMSE	0.422	0.393	0.348
tRMSE	0.422	0.393	0.348
AIC	4117	3585	2690

were not possible to fit with this method because there were too few data points on the far side (trees on the outer edges), or the stems were hidden by dense branches.

The two data sets, the Postex data set and the Laser data set, were combined with a coordinate translation formula defined by 137 preliminary paired tree identities that were linked manually. Final pairing of the tree identities from the respective data sets was conducted by best match due to minimal difference of a) distance between positions, b) height estimation and c) D estimation. Prior to pairing, heights of non-sample trees in the Postex data set, which lacked observation data for this measure, were estimated with a height function fitted to the Simontorp site (see Fagerberg, 2021).

Trees were excluded from the combined data set if the following criteria were not met: a) the tree species is spruce, b) $D > 60$ mm, c) the tree shape is representative (no tendencies to leaning or signs of height development affected by competitors), and d) distance to plot border > 8 m, i.e. all competitors within an 8 m radius are documented in terms of position and diameter (D).

The final data set (Fig. 3) used the tree height estimations from the laser scanning. However, the filtering and reduction of the raw point

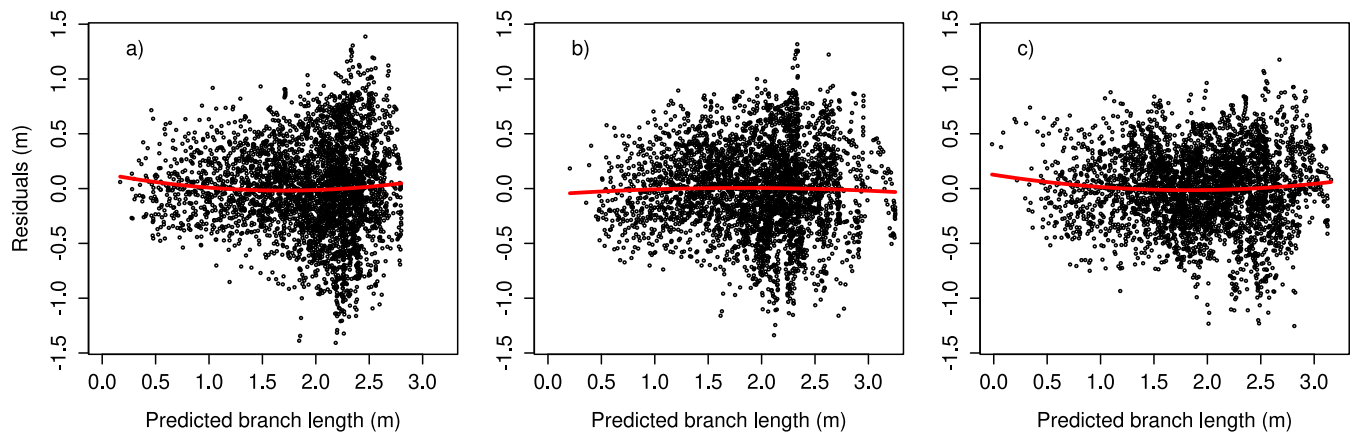


Fig. 6. Horizontal branch length residuals plotted against predicted values for a) model including competition index Bal ($L(Bal, .)$), b) model including crown ratio CR ($L(CR, .)$) and c) complex polynomial model including competition index ($pL(Bal, .)$). Red curves indicate the second-degree polynomial fit.

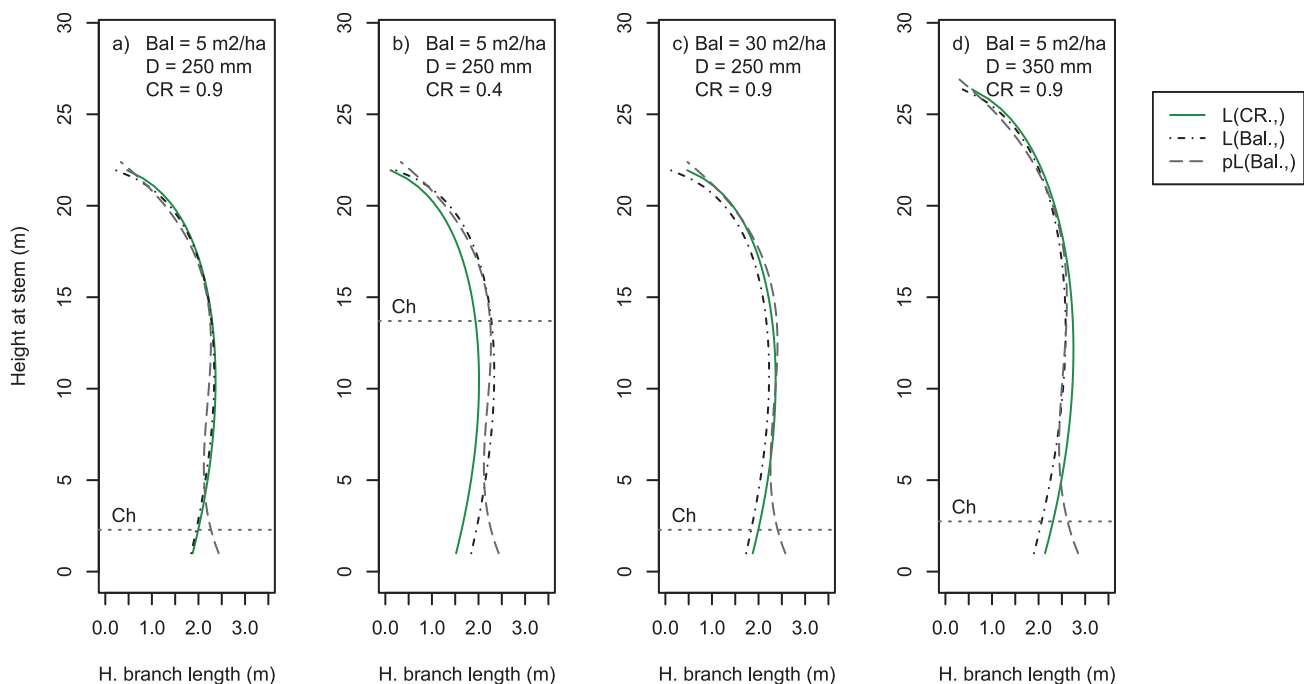


Fig. 7. Predicted horizontal branch lengths with three different models 1) model including crown ratio ($L(CR, .)$), 2) model including competition from larger trees ($L(Bal, .)$), and 3) complex polynomial model including competition from larger trees ($pL(Bal, .)$) displayed with a base setting for the subject tree, i.e. a) basal area of larger competitors within 8 m radius (Bal) = 5 m²/ha, tree diameter at breast height (D) = 250 mm, crown ratio (CR) = 0.9, b) the same base settings but with CR changed to 0.4, c) the same base setting but with Bal changed to 30 m²/ha, and d) the same base setting but with D changed to 350 mm. Ch = height at stem for insertion point of lowest living branch.

cloud resulted in an underestimation of the tree height (Mean = 0.63 m, SD = 0.60 m), because the individual tree tip is only captured by some few sparsely distributed points which might be removed by the filtering. Therefore, the height estimations were adjusted with a bias correction function fitted from a sample of 69 trees in the data set that were also measured manually, see Eq. (1), where y is adjusted height and x is height (dm) from laser scanning observations ($R^2 = 0.994$).

$$y = 1.0095x + 4.5517 \quad (1)$$

Tree positions and D estimations were taken from the Postex data. The maximum distance estimation per octagon section was extracted to represent max horizontal projection per section height (HP_{ht}).

The data were further complemented with variables estimated with static functions from Fagerberg (2021). All formulas referring to Fagerberg (2021) were fitted with data partly or fully from the

Simontorp site. A starting point was that branch age (A) is an important independent variable for the prediction of branch length (Deleuze et al., 1996; Tamm & Mao-Yi, 1987). A can be estimated if height position (h) and ordinal number of individual whorls (W) are known/predicted. Therefore, A was calculated as the difference between whorl ordinal number estimations (W) (Fagerberg, 2021) representing heights Th and h , respectively (Eq. (2)). In this analysis, the corrected laser scan heights represent Th , but a height function ($Th(D)$) was also fitted with the equation by Näslund (1936), which is available in Fagerberg (2021).

$$A_h = W_{Th}(Th_i(D_i)) - W_h(h) \quad (2)$$

The height to crown base observations (Ch) were used to separate living branch observations from non-living observations, and for estimation of the crown ratio (CR). Ch was predicted for eighteen of the sample trees that did not have this information recorded in the field

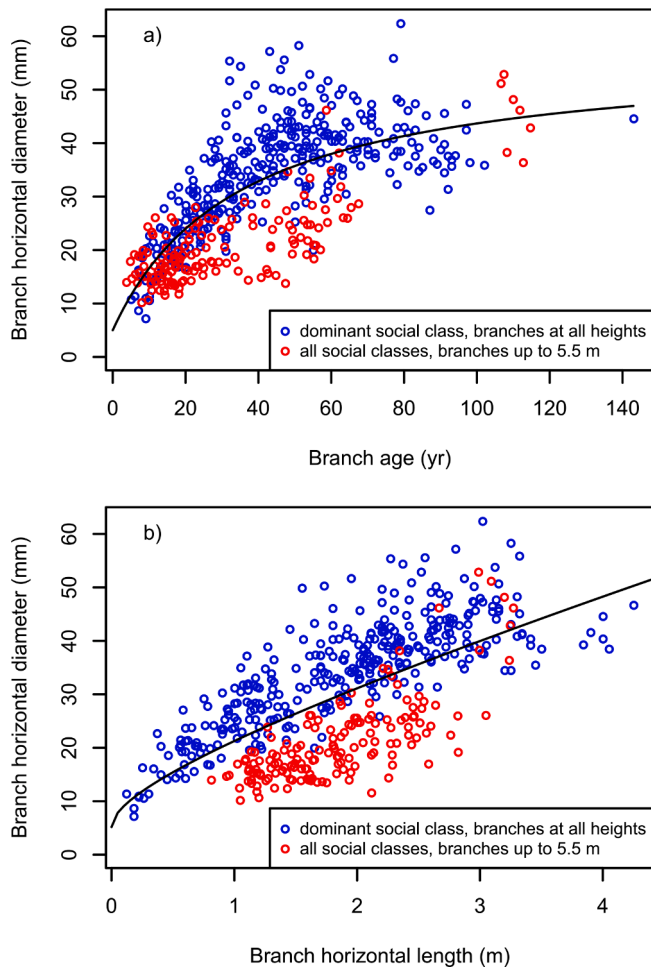


Fig. 8. Branch horizontal diameter observations plotted against a) predicted branch age, and b) observed branch length, presented in two groups defined by tree social class and height positions at the stem. The lines represent fitted models for a) $d(A)$ and b) $d(L)$.

Table 5

Model statistics for four branch diameter models. All models apart from $d(A)$ are multiple linear. $d(A) = 5 + \frac{\alpha A}{b + A}$ AIC = Akaike information criterion. $\alpha = 0.05$. fRMSE = root mean squared error of total sample fit. R^2_{adj} = adjusted R^2 .

	$d(A)$	$\sqrt{d(L)}$	$d(L, D)$	$d(L, A, rd)$
Intercept	5 ^a	2.275	6.318	5.179
a	52.23			
b	35.01			
\sqrt{L}		2.336		
L			3.782	8.647
\sqrt{A}				3.188
D			0.04638	
rd				-24.80
R^2_{adj}		0.458	0.726	0.780
fRMSE	7.49	8.19	4.11	5.26
AIC	3391	1142	888	3041

^a Fixed intercept.

(Formula 1 in Fagerberg (2021)). Then, projection length observations, representing the height positions of the branch tips (ht), needed to be assigned a corresponding height at stem (h) where the insertion point of the branch is assumed to be located. For that purpose, a vertical difference function ($\Delta h(A)$) was used (Fagerberg, 2021). Stem radius over bark (r_h) was calculated with functions from Edgren and Nylinder (1949) (Taper function II, form quotient = 0.6). Finally, based on the

above information, the maximum horizontal branch length (L_h) corresponding to each HP_{ht} observation was calculated (Fig. 4).

Analyses to detect potential outliers among the L_h observations were performed. Observations of trees with crooked stems were excluded if the mean of stem axis deviation from the observed stem section centres (of the top 2 m sections) exceeded 0.3 m. Furthermore, the manual point cloud extraction of the tree individuals required an outlier assessment of individual L_h observations, because of the possibility that points from other individuals were mistakenly included in the extraction. Therefore, if the L_h value exceeded the estimated maximum potential branch length (P , see 3.5 Potential horizontal branch length in Fagerberg (2021)) by >0.7 m, it was regarded as an outlier and removed from the data set ($n = 52$). This limit for outlier detection, was appreciated with sensitivity analysis of P estimation differences due to A estimation error, where the standard deviation of the A error was estimated to be 3.17 years. The remaining dataset consisted of 80 sample trees and 3695 L_h observations (Table 2, Fig. 3).

The manual branch diameter measurements (d) from living branches on standing trees were transferred manually to the main data set, where individual whorls were assigned to the nearest h estimation, and the largest d observation within this/these whorls was selected as the estimation for maximum branch size for that height ($n = 156$, see Table 2).

2.4. Knot size model framework

A framework of linked allometric models was developed to estimate maximum knot size at specified stem heights, see Fig. 5 and Table 3. The framework requires input of subject tree breast height diameter (D_i) together with local competition predictors, either in the format of tree diameters (D_{ci}) and distances to subject tree competitors (R_{ci}), or as an alternative to D_{ci} and R_{ci} , just the estimation of subject tree crown ratio (CR_i), used as a proxy predictor for local competition. The key elements to develop were prediction of branch length as a function of local competition, and prediction of branch diameter as a function of branch length.

Three indexes of local competition were tested for the branch length model: 1) the sum of basal area of larger competitors (Bal), 2) the sum of basal area of all competitors, and 3) a simplified size-distance index derived from Fagerberg et al. (2022). Search radii for all three indexes were 8 m from the subject tree. Furthermore, three different estimations for maximum branch length were tested: 1) horizontal branch length (L), 2) linear branch length between points of the tip and the insertion, and 3) the difference between horizontal branch length and potential branch length in the case of no local competition (Fagerberg, 2021). Initial analysis showed that horizontal branch length (L) and linear branch length displayed the strongest correlations to the tested competition indexes, where L was considered as the simpler and more efficient measure to apply. In addition, the analysis showed that the Bal index had the strongest correlation to L of the tested competition indexes. Therefore, the final analysis focused exclusively on L as the response variable and Bal as a predictor variable for competition.

The requirements for the model fitting were a) slope signs had to correspond to predictor-response correlation, and slope estimation had to meet a significance level of 0.05. All tested predictors were pre-analysed with predictor-response scatterplots and predictors were transformed when applicable to improve the linear correlation. The L model was fitted with fixed multiple linear regression. A , h and relative distance from the treetop (rd) were used as branch level predictors and D , CR and Bal as tree-level predictors. Since A , and to some extent rd , were predicted with D , autocorrelation prohibited reliable inclusion of D as a separate variable when A (or rd) were included. Two of the final L models rely on Bal as the competition predictor, one with linear competition correlation to avoid overfitting and support wider application ($L(Bal, \cdot)$), and one with a more complex polynomial structure ($pL(Bal, \cdot)$). In the second model, four predictors were expressed as three level polynomials (up to third or fourth-degree), which was motivated

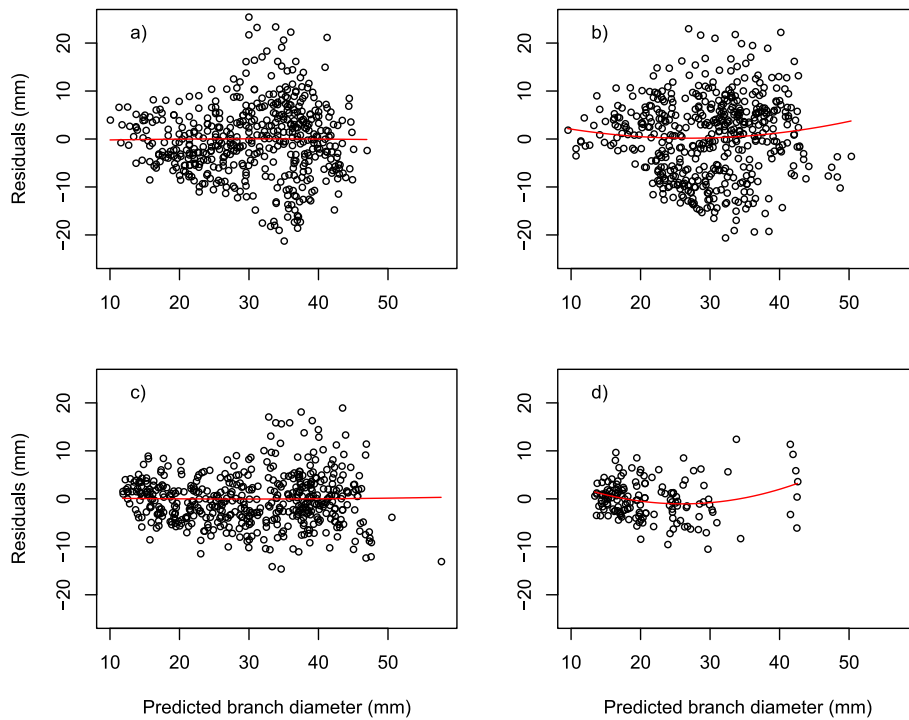


Fig. 9. Horizontal branch diameter residuals of different models with a) branch age as predictor ($d(A)$), b) branch horizontal length as predictor ($d(L)$), c) branch age, horizontal length and relative distance from top as predictors ($d(L, A, rd)$), and d) branch horizontal length and tree diameter as predictors ($d(L, D)$). Red curves indicate the second-degree polynomial fit.

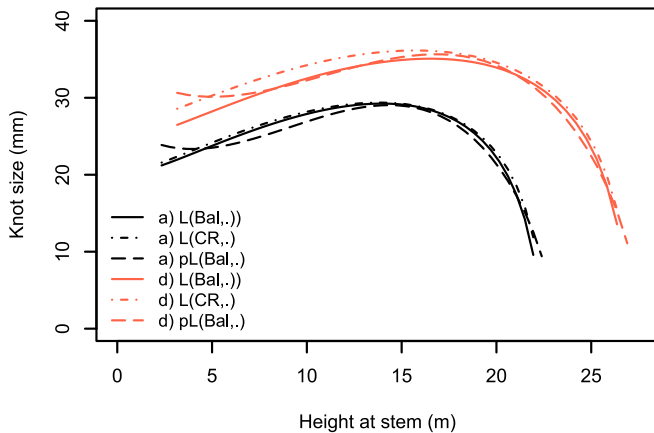


Fig. 10. Knot size predictions with the same branch diameter function ($d(Bal, A, rd)$), but with three different branch length functions, 1) with predictors Bal (basal area from larger trees) branch age (A) and relative distance from top (rd) ($L(Bal, .)$), 2) with the predictors CR, D , and rd ($L(CR, .)$), and 3) a more complex polynomial function with predictors Bal, A , and rd ($pL(Bal, .)$). Two subject tree base settings (red and black) are used, where only tree size differs, a) basal area of larger competitors within 8 m radius (Bal) = 5 m²/ha, tree diameter at breast height (D) = 250 mm, crown ratio (CR) = 0.9, and d) the same base settings as a) but with D changed to 350 mm (see also Fig. 7a, that uses the same settings).

by tendencies of sigmoidal shapes of the predictor-response relationships. The third model presented was based on CR as the predictor representing competition ($L(CR, .)$).

The reference tree data set was used together with the main data set for fitting models for branch diameter (d) ($n = 493$). Four separate models were fitted: 1) a non-linear model with A as predictor and intercept set to 5 ($d(A)$) (the fixed 5 mm intercept is determined by the approximate minimum possible branch diameter), 2) a simple linear model with L as predictor ($\sqrt{d}(L)$), 3) a multiple linear model with L, A

Table 6

Branch diameter root mean squared errors (mm) from model framework validation with different combinations of branch length and branch diameter models, tested on living branch observations from the test site up to 5.5 m stem height ($n = 190$, distributed on 47 trees). $d()$ = branch diameter model, $L(CR, .)$ = branch length model based on crown ratio, $L(Bal, .)$ = branch length model based on basal area of larger trees, A = branch age, D = tree diameter, and $pL()$ = complex polynomial branch length model.

Model combinations	RMSE
$d(L(CR, .), A, rd)$	5.70
$d(L(CR, .), D)$	4.57
$d(L(CR, .))$	8.95
$d(L(Bal, .), A, rd)$	5.83
$d(L(Bal, .), D)$	4.65
$d(L(Bal, .))$	9.89
$d(pL(Bal, .), A, rd)$	5.68
$d(pL(Bal, .), D)$	4.55
$d(pL(Bal, .))$	9.70
$d(A)$	9.44

and rd as predictors ($d(L, A, rd)$), and 4) a multiple linear model with L and D as predictors ($d(L, D)$). The $\sqrt{d}(L)$ model was scaled by square root transformation of both the predictor and the response. The $d(L, D)$ model was fitted with values representative for the butt log (maximum length 5.5 m) since the available data only covered this part of the stem.

To calculate knot size (K) from branch diameter (d), the vertical branch angle (α) was needed. α at stem insertion was estimated with a linear function of A , where α is the angle measured from the horizontal plane (Fagerberg, 2021). Then, knot size (K_h), at the position of the stem insertion h may be calculated using trigonometric principles, assuming that the cross-sectional area of the branch is perfectly circular. The above assumptions translate into equation (3):

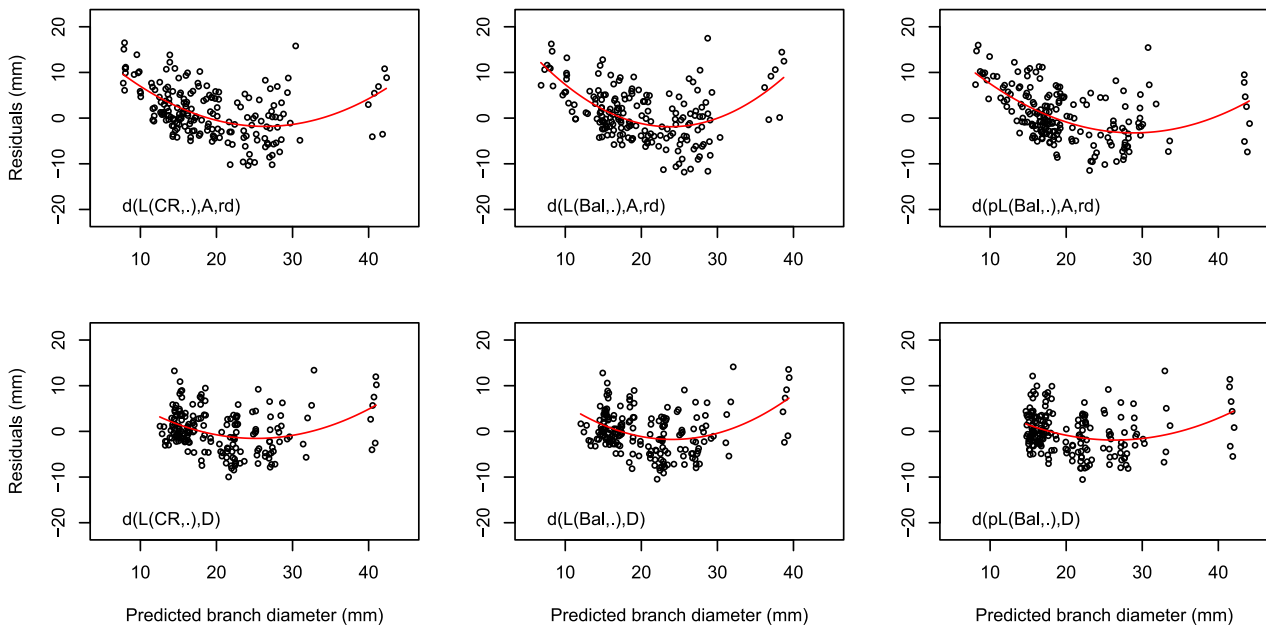


Fig. 11. Branch diameter residuals from model framework validation with the best performing combinations of branch length and branch diameter models, tested on living branch observations from the test site up to 5.5 m stem height ($n = 190$, distributed on 47 trees). $d(\dots)$ = branch diameter model, $L(CR, \cdot)$ = branch length model based on crown ratio, $L(Bal, \cdot)$ = branch length model based on basal area of larger trees, $pL(\cdot)$ = complex polynomial branch length model, A = branch age, D = tree diameter, and rd = relative distance from treetop. Red curves indicate the second-degree polynomial fit.

$$K_h = \frac{d_h - 2t}{\cos(\alpha)} = \frac{d_h - 2t}{\cos(-24.07 + 0.357A_h)} \quad (3)$$

where t is branch bark thickness (mm). The second expression includes the function for branch angle from Fagerberg (2021). In the knot size predictions, t was assumed to be 1.5 mm.

2.5. Validation

All fitted models are presented with estimates of Akaike’s information criterion (AIC). Linear models are presented with statistics of adjusted R^2 . All L models were tested with ten-fold cross-validation and mean values of test root mean square error (tRMSE) were compared with corresponding values from the model fit (fRMSE). The d -models were evaluated mainly using the fRMSE estimates and the residual scatterplot patterns. Residuals were calculated by subtracting the estimated value from the observed value.

A model framework validation was carried out by testing the different framework combinations on the 190 branch diameter observations available from the combined data set before outlier removal. Some 156 of these observations had been used in the calibration data for the d model. Horizontal branch diameter was predicted with all L and d model combinations ($n = 10$, see Fig. 5, where two of the framework combinations are shown). If total tree height was larger than the asymptote in the W_{Th} model in these calculations, then height was assumed equal to the asymptote, i.e. $W_{Th} = 275$ (representing the total age of the tree). The CR was predicted by use of crown base (Ch) as a function of D_i (see 3.4, model 1, in Fagerberg, 2021). It was tested to use a corresponding Ch function that also includes a predictor for basal area competition, but the difference in prediction accuracy was negligible. Consequently, the local competition impact was assumed to be statically correlated with D_i when L is predicted with $L(CR, \cdot)$, but for combinations based on $L(Bal, \cdot)$, competition impact was ultimately determined by diameters at breast height of larger competitors (D_{ci}) and distances to these competitors (R_{ci}).

3. Results

3.1. Branch length models

The statistical polynomial model $pL(Bal, \cdot)$ is the best performing model in terms of prediction statistics and minimized heteroscedasticity (Table 4, Fig. 6). The competition model with the simpler model format ($L(Bal, \cdot)$) displayed lower prediction accuracy. In this case, the heteroscedastic tendencies increased and the prediction range was reduced relative to the other models. The third model alternative ($L(CR, \cdot)$) performed in between the other two models according to the fit statistics. The visual prediction behaviour of the models when the input settings are allowed to vary (Fig. 7), indicates that $L(Bal, \cdot)$ is slightly more sensitive than $pL(Bal, \cdot)$ to the competition index Bal .

3.2. Branch diameter models

The scatterplot with branch observation data (Fig. 8b) demonstrates that the relationship between L_h and d is dependent on the insertion point height (h), where branches located within butt log heights (0–5.5 m) indicate a more linear relationship (red markers). The $d(L, D)$ model, which is fitted on this lower section of the stem, displays the lowest RMSE value (4.11 mm) (Table 5). The three models calibrated for the full stem length show higher RMSE values the simpler the model formula is, from 5.26 mm ($d(L, A, rd)$) to 8.19 mm ($\sqrt{d(L)}$). The $d(L, A, rd)$ model has the most reliable residual pattern and the highest R^2 estimate compared to the other models (Fig. 9).

3.3. Knot size prediction

The choice of branch diameter model strongly influenced the knot size prediction when the modelling framework was tested on mature trees ($D = 250$ and 350 mm), see Appendices, Fig. A1. In this case, the predictions from the $d(L, A, rd)$ and $d(L, D)$ models displayed the highest degree of coherence. In the same test context, all three branch length models also expressed a high level of coherence, see Fig. 10. When different levels of competition were simulated with the $L(Bal, \cdot)$ model,

the result showed that the *Bal* impact on knot size is relatively small (Appendices, Fig. A2), never exceeding 2 mm difference although the competition increased from 5 m²/ha to 30 m²/ha (while the remaining input was kept constant).

3.4. Validation

The root mean squared error (RMSE) was estimated to be 4.6–4.7 mm for model combinations covering butt log heights and 5.7–5.8 mm for the remaining whole-tree model combinations. Based on the validation data, the most reliable model combination for knot size prediction in the butt log is $d(pL(Bal, \cdot), D)$, but the simpler combination based on CR ($d(L(CR, \cdot), D)$) performs at a comparable level (Table 6, Fig. 11). Concerning the combinations that are applicable to the whole stem, the $d(pL(Bal, \cdot), A, rd)$ model proved to be the most reliable alternative. Here too, the CR alternative ($d(L(CR, \cdot), A, rd)$) performed at a similar level. However, the residual plot indicates that knots below 15 mm have a high risk of being overestimated even by the best performing whole stem combination ($d(pL(Bal, \cdot), A, rd)$).

4. Discussion

4.1. Horizontal branch length

The analyses and results indicate that the relationship between linear estimates of local competition and horizontal branch length is weak. The competition index based on basal area of larger competitors (*Bal*) was the only one of tested indexes that showed a significant negative correlation with branch length. Even the *Bal* index did not improve the prediction accuracy of branch length compared to the model alternative where competition was described with *CR*, indicating that there is a cost in the explained variation related to the incorporation of one simple linear predictor for local competition. However, when the competition component was allowed to be non-linear and multiple ($pL(Bal, \cdot)$), it supported a higher degree of explained variation. Thus, with a properly designed formula, *Bal* can contribute to model performance, albeit to a limited extent, provided that the required detailed data is available. In situations where local competition impact is not a main focus or where time or logistic constraints do not permit gathering competition data, the $L(CR, \cdot)$ model is sufficient. Similar simple model approaches have been used before e.g. by Roeh and Maguire (1997), who developed crown profile models for Douglas fir based on endogenous whole tree variables restricted to input of tree diameter, tree height and crown length.

The competition index analysis supports the results from previous research (Purves et al., 2007; Vincent & Harja, 2008) that asymmetric indexes are better suited for prediction of crown shape than symmetric alternatives. The explanatory power of the competition index could possibly be improved with more specific input e.g. from variables such as tree social class (Pretzsch & Rais, 2016), azimuthal orientation (Rouvinen & Kuuluvainen, 1997) and distance to competitors for the specified branch direction (Deleuze et al., 1996).

The visualization plots (Figs. 7 and 10) indicate that the $pL(Bal, \cdot)$ model might be less reliable for branches close to ground and/or with *CR* values above 0.85, since the curves show increasing deviation with lower stem heights. For this reason, butt log simulation poses a risk of overestimation with this model, especially for large trees with long crowns (cf. Fig. 11).

4.2. Branch horizontal diameter

The visual results shown in Figs. 10 and 11 demonstrate that the choice of diameter model has a greater impact on the knot size prediction than the choice of branch length model. Nevertheless, the applicability of the individual d -models depends on the situation because each have different limitations. The branch age function ($d(A)$) can be

expected to be relevant for small trees and younger branches from the topmost 5 m of the crown, since branches in this section are nearly independent of tree age and degree of competition (Kantola & Mäkelä, 2004). Accordingly, the model also showed increasing residual variation with increasing branch age (Fig. 9a). However, in this analysis, the variation increases with tree size (D) since the estimation error of A follows the increasing errors in the W prediction when trees are larger and top whorl distances become smaller. Therefore, height estimation error increases with tree size, along with increased W prediction error per height error unit, causing the A estimation error to increase exponentially with tree size.

To some extent, the function ($d(L)$) is complementary to the $d(A)$ model because branch length tends to maintain explanatory capacity with older branches. This effect is utilized in the $d(L, D)$ model which covers the butt log section of the stem. This model alternative also displayed the highest presented simulation accuracy. However, if one single model is to be used for a general application to trees of different sizes with coverage of all height positions, the $d(L, A, rd)$ model is the obvious choice due to its stable residual variation. In the end, the performance of this model is mainly dependent on the availability and quality of the input data for the predictors L and A , both of which are demanding variables to handle in the data management.

It is possible that residual variation could be reduced by including additional variables such as height of insertion (h) and tree social position (Seifert, 2003). Regarding the impact of h , it was tested to add a second-degree polynomial expression of h . This improved the RMSE considerably, but even so this model alternative was not included because the branch data is not represented by social classes other than dominant trees for branches above 5.5 m height. Thus, the resulting regression coefficients would possibly not have been representative for lower social classes.

4.3. Validation and application

The model framework with its current specification is valid for sites with growing conditions similar to the calibration data, i.e. uneven-sized Norway spruce dominated fertile sites in southern Sweden. Application to comparable site properties would likely also be reliable since site fertility has been shown to have low significance for branch prediction (Mäkinen et al., 2003). The preferred model combination for individual applications can be selected according to context, available input data, study aim and scope. In general, the validation test results give guidance to the choice of model combination, although it is difficult to draw a firm conclusion about which alternative is most suitable for application to butt logs. The $d(L, D)$ model displays convincing residuals, however, the validity for that model is tentative since training and test sets were limited and overlapped by 82%. The flexible modular format of the framework makes it possible to adjust to different circumstances e.g. by extending the calibration ranges or improving the function formats for specific sub-models. In some cases, there are other models available that can be incorporated to the benefit of the accuracy and applicability of the framework, e.g. the hight to crown base model dependent on local competition, presented by Bianchi et al. (2020b).

The modelling concept where crown or competitive status is linked with knot size through a chain of allometric models can also be applied to even-sized conditions, provided that different sub-models suitable for homogenous stands are used. In particular, the functions covering the impact from local competition are preferably based on predictors for total basal area and stand development stage instead of the asymmetric competition index of *Bal* (Bianchi et al., 2020b). Alternatively, the competition index is omitted entirely and the crown shape in the more homogeneous structure is described directly with internal tree variables (Moberg, 2001; Mäkinen et al., 2003). Furthermore, the presented whorl number function (W), will be less reliable in even-sized stands depending on the faster height growth of smaller trees compared to uneven-sized stands. Reported RMSE values for corresponding

allometric models developed for even-sized stands are lower compared to this study, 5.4 mm (Moberg, 2006), 3.2 mm (Mäkinen et al., 2003) and 3.7 mm (Colin & Houllier, 1991). This is likely a consequence of the heterogeneous stand structure in this study causing more variation in crown shape (Kumpu et al., 2020) that is difficult to predict.

5. Conclusions

A novel model framework was presented for simulation of largest knot size in uneven-sized Norway spruce stands. With this tool, the impact of selective cutting on external stem quality can be incorporated in management simulations. Since the size of knots is decisive for timber grading, and ultimately impacts the economic output from management, these models facilitate detailed profitability evaluations of silvicultural alternatives. Different model combinations are proposed depending on the prediction aim and format of the available local competition input, i. e. whether the tree data contains tree positions or not. The modular format enables further development of separate sub-components to create locally adapted framework versions outside the current calibration range. In general, simulations with the competition-dependent model combinations indicate that the impact from local competition on knot size is rather limited.

Funding

This work was supported by the Swedish Research Council [grant number 2015-13600-30399-30], the Foundation Seydlitz MP Bolagen [Uppskattning av virkeskvalité genom markbaserad laser, 2018].

CRedit authorship contribution statement

N. Fagerberg: Conceptualization, Data curation, Formal analysis, Investigation, Methodology, Validation, Visualization, Writing – original draft, Writing – review & editing. **S. Seifert:** Data curation, Visualization. **T. Seifert:** Conceptualization, Data curation, Methodology, Supervision. **P. Lohmander:** Conceptualization, Methodology, Supervision. **A. Alissandrakis:** Data curation, Software, Supervision, Visualization. **B. Magnusson:** Data curation, Visualization. **J. Bergh:** Supervision, Writing – review & editing. **S. Adamopoulos:** Conceptualization, Supervision, Writing – review & editing. **M.K.-F. Bader:** Formal analysis, Writing – review & editing.

Declaration of Competing Interest

The authors declare that they have no known competing financial interests or personal relationships that could have appeared to influence the work reported in this paper.

Data availability

The data that support the findings of this study are openly available in the public repository Swedish National Data Service at <https://doi.org/10.5878/f7vh-9e91>, reference number 2022-144-1.

Acknowledgements

The authors are grateful for the good cooperation with the forest owner of the Simontorp site, Anders Blidberg. Important assistance with field measurements was obtained from Rutger Nicklasson, Oscar Jönsson and Göran Snygg. Grace Jones helped with the language check.

Appendix A

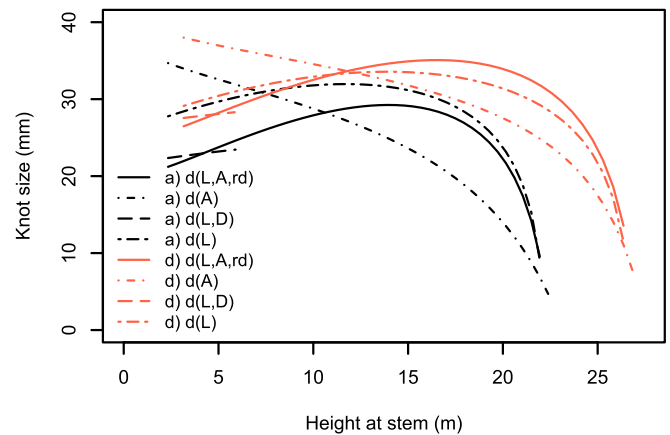


Fig. A1. Knot size predictions with one branch length function ($L(Bal, \cdot)$), but with four different branch diameter functions, 1) with predictors branch length, branch age and relative distance from top ($d(L, A, rd)$), 2) with the predictor branch age ($d(A)$), 3) with predictors branch length and tree diameter ($d(L, D)$) (height at stem >5.5 m are values outside the calibration range), and 4) with predictor branch length ($d(L)$). Two subject tree base settings (red and black) are used, where only tree size differs, a) basal area of larger competitors within 8 m radius (Bal) = 5 m²/ha, tree diameter at breast height (D) = 250 mm, crown ratio (CR) = 0.9, and d) the same base setting as in a) but with D changed to 350 mm (see also Fig. 7a, that uses the same settings).

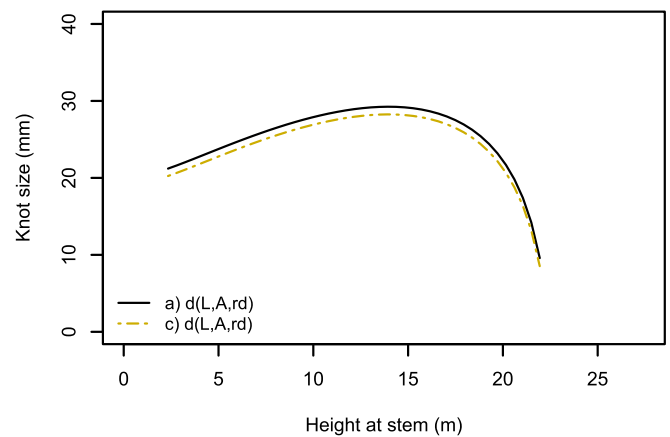


Fig. A2. Knot size predictions under bark, with two subject tree base settings (beige and black) where only local competition differs, a) basal area of larger competitors within 8 m radius (Bal) = 5 m²/ha, tree diameter at breast height (D) = 250 mm, crown ratio (CR) = 0.9, and b) the same base settings but with Bal changed to 30 m²/ha (see also Fig. 7a and Fig. 11, that uses the same settings). Knot sizes are predicted with the branch length function ($L(Bal, \cdot)$) which depends on competition as basal area of larger competitors, and with the branch diameter function ($d(L, A, rd)$) which depends on branch length, branch age and relative distance from top. Curves are displayed from the height of lowest living branch insertion point (Ch).

References

- Anon. (2014). Grading of sawlogs of pine and spruce. In *SDCs instructions for timber measurement*. (pp. 10). Sundsvall: Skogsbrukets datacentral, Sweden.
- Baño, V., Arriaga, F., Guaita, M., 2013. Determination of the influence of size and position of knots on load capacity and stress distribution in timber beams of *Pinus sylvestris* using finite element model. *Biosyst. Eng.* 114 (3), 214–222. <https://doi.org/10.1016/j.biosystemseng.2012.12.010>.
- Bianchi, S., Huuskonen, S., Siipilehto, J., Hynynen, J., 2020a. Differences in tree growth of Norway spruce under rotation forestry and continuous cover forestry. *Forest Ecol. Manag.* 458, 117689 <https://doi.org/10.1016/j.foreco.2019.117689>.
- Bianchi, S., Siipilehto, J., Hynynen, J., 2020b. How structural diversity affects Norway spruce crown characteristics. *For. Ecol. Manag.* 461, 117932 <https://doi.org/10.1016/j.foreco.2020.117932>.
- Björklund, L. (2021). *Visionseminarium om kvaliteten på sågtimmer - minnesanteckningar och slutsatser, Sigtuna 15-16 Nov (in Swedish)*. Rådet för mätning och redovisning, Sågtimmerkommittén, Biometria, Sweden.
- Colin, F., Houllier, F., 1991. Branchiness of Norway spruce in north-eastern France: modelling vertical trends in maximum nodal branch size. *Ann. Sci. For.* 48 (6), 679–693.
- Colin, F., Houllier, F., 1992. Branchiness of Norway spruce in northeastern France: predicting the main crown characteristics from usual tree measurements. *Ann. Sci. For.* 49 (5), 511–538.
- Deleuze, C., Herve, J.-C., Colin, F., Ribeyrolles, L., 1996. Modelling crown shape of *Picea abies*: spacing effects. *Can. J. For. Res.* 26 (11), 1957–1966. <https://doi.org/10.1139/x26-221>.
- Edgren, V., Nylinder, P. (1949) Funktioner och tabeller för bestämning av avsmalning och formkvot under bark för tall och gran i norra och södra Sverige (in Swedish). In: *Meddelanden från Statens skogsforskningsinstitut*, 38:7. Statens skogsforskningsinstitut, Sweden.
- Fagerberg, N., Olsson, J.-O., Lohmander, P., Andersson, M., Bergh, J., 2022. Individual-tree distance-dependent growth models for uneven-sized Norway spruce. *Forestry* 1–13. <https://doi.org/10.1093/forestry/cpac017>.
- Fagerberg, N. (2021). Some specific sub-models for simulation of uneven-sized Norway spruce: within contexts of forest management, stem quality and tree growth. In: *Workreport*. Linnaeus University, Department of Forestry and Wood Technology.
- Geburek, T., Robitschek, K., Milasowszky, N., 2008. A tree of many faces: Why are there different crown types in Norway spruce (*Picea abies* [L.] Karst.)? *Flora Morphol. Distrib. Funct. Ecol. Plants* 203 (2), 126–133. <https://doi.org/10.1016/j.flora.2007.01.003>.
- Gilmore, D.W., Seymour, R.S., 1997. Crown architecture of *Abies balsamea* from four canopy positions. *Tree Physiol.* 17 (2), 71–80. <https://doi.org/10.1093/treephys/17.2.71>.
- Grubb, P.J., 1998. A reassessment of the strategies of plants which cope with shortages of resources. *Perspect. Plant Ecol. Evol. Syst.* 1 (1), 3–31. <https://doi.org/10.1078/1433-8319-00049>.
- Hägglund, B., Lundmark, J.-E., 1977. Site index estimation by means of site properties. *Stud. For. Suec* 138, 1–38.
- Hasenauer, H., Monserrud, R.A., 1996. A crown ratio model for Austrian forests. *Forest Ecol. Manag.* 84 (1–3), 49–60. [https://doi.org/10.1016/0378-1127\(96\)03768-1](https://doi.org/10.1016/0378-1127(96)03768-1).
- Houllier, F., Leban, J.-M., Colin, F., 1995. Linking growth modelling to timber quality assessment for Norway spruce. *Forest Ecol. Manag.* 74 (1), 91–102. [https://doi.org/10.1016/0378-1127\(94\)03510-4](https://doi.org/10.1016/0378-1127(94)03510-4).
- Johansson, K., 1992. Effects of initial spacing on the stem and branch properties and graded quality of *Picea abies* (L.) karst. *Scand. J. For. Res.* 7 (1–4), 503–514. <https://doi.org/10.1080/02827589209382743>.
- Johansson, C.-J., 2003. Grading of timber with respect to mechanical properties. In: Thelandersson, S., Larsen, H. (Eds.), *Timber Engineering*. John Wiley & Sons, West Sussex, pp. 23–43.
- Kantola, A., Mäkelä, A., 2004. Crown development in Norway spruce [*Picea abies* (L.) Karst.]. *Trees* 18 (4), 408–421. <https://doi.org/10.1007/s00468-004-0319-x>.
- Kern, K.G., 1966. *Wachstum und Umweltfaktoren im Schlag-und Plenterwald (Growth and environmental factors of a selection forest)* (in German). Bayerischer Landwirtschaftsverlag, München Basel Wien.
- Krajicek, J.E., Brinkman, K.A., Gingrich, S.F., 1961. Crown competition—a measure of density. *For. Sci.* 7 (1), 35–42.
- Kumpu, A., Piispanen, R., Berninger, F., Saarinen, J., Mäkelä, A., 2020. Biomass and structure of Norway spruce trees grown in uneven-aged stands in southern Finland. *Scand. J. For. Res.* 35 (5–6), 252–261. <https://doi.org/10.1080/02827581.2020.1788138>.
- Macdonald, E., Gardiner, B., Mason, W., 2009. The effects of transformation of even-aged stands to continuous cover forestry on conifer log quality and wood properties in the UK. *Forestry* 83 (1), 1–16. <https://doi.org/10.1093/forestry/cpp023>.
- Macdonald, E., Hubert, J., 2002. A review of the effects of silviculture on timber quality of Sitka spruce. *Forestry* 75 (2), 107–138. <https://doi.org/10.1093/forestry/75.2.107>.
- Madgwick, H., Tamm, C., Mao-Yi, F., 1986. Crown development in young *Picea abies* stands. *Scand. J. For. Res.* 1 (1–4), 195–204. <https://doi.org/10.1080/02827588609382411>.
- Mäkinen, H., Ojansuu, R., Sairanen, P., Yli-Kojola, H., 2003. Predicting branch characteristics of Norway spruce (*Picea abies* (L.) Karst.) from simple stand and tree measurements. *Forestry* 76 (5), 525–546. <https://doi.org/10.1093/forestry/76.5.525>.
- Man, R., Loeffers, V.J., 1999. Are mixtures of aspen and white spruce more productive than single species stands? *For. Chron.* 75 (3), 505–513. <https://doi.org/10.5558/tfc75505-3>.
- Mitchell, K.J., 1975. *Dynamics and simulated yield of Douglas-fir*. *For. Sci.* 21 (suppl.1).
- Mitsuhashi, K., Poussa, M., Puttonen, J., 2008. Method for predicting tension capacity of sawn timber considering slope of grain around knots. *J. Wood Sci.* 54 (3), 189–195. <https://doi.org/10.1007/s10086-007-0941-5>.
- Moberg, L., 2001. Models of internal knot properties for *Picea abies*. *Forest Ecol. Manag.* 147 (2–3), 123–138. [https://doi.org/10.1016/S0378-1127\(00\)00471-0](https://doi.org/10.1016/S0378-1127(00)00471-0).
- Moberg, L., 2006. Predicting knot properties of *Picea abies* and *Pinus sylvestris* from generic tree descriptors. *Scand. J. For. Res.* 21 (S7), 49–62. <https://doi.org/10.1080/14004080500487011>.
- Näslund, M. (1936) Skogsförsöksanstaltens gallringsförsök i tallskog (in Swedish). In: *Meddelanden från statens skogsförsöksanstalt*, Häfte 29: Swedish Institute of Experimental Forestry.
- Oscarsson, J., Olsson, A., Enquist, B., 2012. Strain fields around knots in Norway spruce specimens exposed to tensile forces. *Wood Sci. Technol.* 46 (4), 593–610. <https://doi.org/10.1007/s00226-011-0429-8>.
- Ottorini, J., 1991. Growth and development of individual Douglas-fir in stands for applications to simulation in silviculture. *Ann. Sci. For.* 48 (6), 651–666. <https://doi.org/10.1051/forest:19910604>.
- Pretzsch, H., Rais, A., 2016. Wood quality in complex forests versus even-aged monocultures: review and perspectives. *Wood Sci. Technol.* 50 (4), 845–880. <https://doi.org/10.1007/s00226-016-0827-z>.
- Purves, D.W., Lichstein, J.W., Pacala, S.W., Rees, M., 2007. Crown plasticity and competition for canopy space: a new spatially implicit model parameterized for 250 North American tree species. *PLoS One* 2 (9), e870. <https://doi.org/10.1371/journal.pone.0000870>.
- Roeh, R.L., Maguire, D.A., 1997. Crown profile models based on branch attributes in coastal Douglas-fir. *Forest Ecol. Manag.* 96 (1–2), 77–100. [https://doi.org/10.1016/S0378-1127\(97\)00033-9](https://doi.org/10.1016/S0378-1127(97)00033-9).
- Rouvain, S., Kuuluvainen, T., 1997. Structure and asymmetry of tree crowns in relation to local competition in a natural mature Scots pine forest. *Can. J. For. Res.* 27 (6), 890–902. <https://doi.org/10.1139/x97-012>.
- Schütz, J.-P. (1997). *Sylviculture 2: la gestion des forêts irrégulières et mélangées (Silviculture 2. Management of uneven-aged and mixed forests)* (In French) (Vol. 2). Lausanne: Presses Polytechniques et Universitaires Romandes.
- Seifert, T., 2003. *Integration von Holzqualität und Holzsortierung in behandlungssensitive Waldwachstumsmodelle (Integration of wood quality, grading and bucking in forest growth models sensitive to silvicultural treatment)*. Technische Universität München, Germany. Ph.D. thesis.
- Seifert, T. (1999). *Modelling wood quality of Norway spruce (Picea abies) depending on silvicultural treatment*. Paper presented at the Proceedings of the Third IUFRO, La Londe-Les-Maures.
- Skatter, S., Kucera, B., 1998. The cause of the prevalent directions of the spiral grain patterns in conifers. *Trees* 12 (5), 265–273. <https://doi.org/10.1007/s004680050150>.
- Tamm, C., Mao-Yi, F., 1987. Predicting branch and needle growth of spruce (*Picea abies* (L.) karst.) from easily measurable tree parameters. II: Branch weight. *Acta Oecologica, Oecologia Plant* 8 (1), 21–236.
- Vestøl, G.I., Colin, F., Loubère, M., 1999. Influence of progeny and initial stand density on the relationship between diameter at breast height and knot diameter of *Picea abies*. *Scand. J. For. Res.* 14 (5), 470–480. <https://doi.org/10.1080/02827589950154177>.
- Vieilledent, G., Courbaud, B., Kunstler, G., Dhôte, J.-F., Clark, J.S., 2010. Individual variability in tree allometry determines light resource allocation in forest ecosystems: a hierarchical Bayesian approach. *Oecologia* 163 (3), 759–773. <https://doi.org/10.1007/s00442-010-1581-9>.
- Vincent, G., Harja, D., 2008. Exploring ecological significance of tree crown plasticity through three-dimensional modelling. *Ann. Bot.* 101 (8), 1221–1231. <https://doi.org/10.1093/aob/mcm189>.
- Weiner, J., Thomas, S.C., 1986. Size variability and competition in plant monocultures. *Oikos* 47, 211–222. <https://doi.org/10.2307/3566048>.
- Williams, J.M., Fridley, K.J., Cofer, W.F., Falk, R.H., 2000. Failure modeling of sawn lumber with a fastener hole. *Finite Elem. Anal. Des.* 36 (1), 83–98. [https://doi.org/10.1016/S0168-874X\(00\)00010-X](https://doi.org/10.1016/S0168-874X(00)00010-X).